

Schottky barrier heights and interface chemistry in Ag, In, and Al overlayers on GaP(110)

M. Alonso, R. Cimino, Ch. Maierhofer, Th. Chassé, W. Braun, and K. Horn

Citation: *Journal of Vacuum Science & Technology B: Microelectronics Processing and Phenomena* **8**, 955 (1990); doi: 10.1116/1.584949

View online: <https://doi.org/10.1116/1.584949>

View Table of Contents: <https://avs.scitation.org/toc/jvm/8/4>

Published by the [American Institute of Physics](#)

ARTICLES YOU MAY BE INTERESTED IN

Schottky barrier height measurements of Cu/Si(001), Ag/Si(001), and Au/Si(001) interfaces utilizing ballistic electron emission microscopy and ballistic hole emission microscopy
AIP Advances **3**, 112110 (2013); <https://doi.org/10.1063/1.4831756>

Schottky barrier heights and interface chemistry in Ag, In, and Al overlayers on GaP(110)

M. Alonso, R. Cimino,^{a)} Ch. Maierhofer, Th. Chassé,^{b)} W. Braun,^{c)} and K. Horn
Fritz-Haber-Institut der Max-Planck-Gesellschaft, D-1000 Berlin 33, West Germany

(Received 30 January 1990; accepted 16 April 1990)

We have carried out a study of the chemical reaction of silver, indium, and aluminium layers with cleaved GaP(110) surfaces using photoemission with synchrotron radiation. Core level photoelectron spectra show that silver and indium overlayers do not cause an interface reaction with GaP(110). The deposition of Al, on the other hand, leads to an extensive exchange reaction which also proceeds at low temperature, although influenced by changes in overlayer growth morphology. Surface band bending induced by the metallic overlayers was investigated as a function of deposition for *n*- and *p*-type material. In contrast to earlier findings, almost identical Schottky barrier heights for In and Ag deposition are obtained, despite the large difference in work function between these two metals. Results for Al also suggest that a small range of pinning positions is responsible for the Schottky barrier heights for junctions of these metals with GaP(110). We find that large peak shifts due to a surface photovoltage induced by the photoemission light source affect the determination of the Schottky barrier heights. This and other possible reasons for the discrepancy with earlier work are discussed.

I. INTRODUCTION

The possibility to characterize chemical interactions between a metal and a semiconductor surface, and to simultaneously determine the Schottky barrier height, has made photoelectron spectroscopy the preferred technique to study Schottky barrier formation on a microscopic scale.¹⁻³ Here we report experiments with indium, silver, and aluminium overlayers on cleaved GaP(110) surfaces, in order to compare the chemical reactions when unreactive (In, Ag) as well as reactive (Al) metals are deposited. We complement the studies of interface chemistry by a detailed investigation of surface Fermi level position as a function of metal layer thickness at both room and low substrate temperatures. The temperature-dependent experiments are aimed at understanding the influence of changes in the morphology of the overlayer on the evolution of the Fermi level pinning, and on the extent of interface reaction. The behavior of metals on GaP(110) is also interesting for another reason: while for most metal-semiconductor systems the Schottky barrier ϕ_b has been found to be largely independent of the deposited metal, recent reports have⁴ indicated that on this surface, ideal Schottky behavior, i.e., a linear dependence of ϕ_b on metal work function, has been found. Such behavior may add to an understanding of the substrate-dependent parameters which influence ϕ_b . In this study, we did not find the Schottky behavior reported earlier. However, we found evidence for photon-induced nonequilibrium processes which are of wider interest beyond the investigation of a single metal-semiconductor system. These processes may also affect the determination of surface band bending by photoemission in other metal-semiconductor systems.

II. EXPERIMENTAL

Data were recorded using two commercial angle-resolving photoelectron spectrometers (ARIES by VSW Ltd., and ADES 400 by VG Scientific, Great Britain) equipped with

moveable hemispherical electron energy analyzers. The chambers also contained a low energy electron diffraction (LEED) optics, a cleavage device, and several metal evaporators. Data were recorded on the TGM (toroidal grating monochromator) 5 and 6 on the wiggler/undulator beamline as well as on the 1 m Seya-Namioka monochromator beamline at the BESSY (Berliner Speicherring-Gesellschaft für Synchrotronstrahlung) storage ring in Berlin. The TGM monochromator gives access to a high flux of photons from about 30 to 300 eV, with resolution $E/\Delta E \sim 1000$ under normal operating conditions. The electron analyzer was operated such that the overall resolution was about 60 meV at a photon energy of 55 eV for most studies; some experiments on the 1 m Seya were carried out with a resolution of about 200 meV. Spectra were recorded under 40 to 50 deg angle of incidence of the light, and normal emission (analyzer half-angle about 2 deg). Indium and silver were evaporated from a basket made of tungsten mesh, which was heated by 0.3 mm tungsten wire; this arrangement gave reproducible evaporation rates, at operating pressures of 1×10^{-10} mbar and below. Aluminium was evaporated from a molecular beam epitaxy cell of our own design,⁵ and operated at a temperature of about 900 °C at a pressure of about 3×10^{-10} mbar. Prenchnotched bars of GaP (undoped, carrier concentration of typically 3×10^{-16} cm⁻³, *n*-(sulphur)-doped, carrier concentration of typically 2×10^{17} to 2×10^{18} cm⁻³, and *p*-(zinc) doped, carrier concentration 1.7 to 5.8×10^{17}) were cleaved *in situ*, at an operating pressure of 5×10^{-11} mbar. The crystals were mounted in ohmic contact on a specimen holder which allowed cooling to about 100 K using liquid nitrogen. In several experiments, two crystals, doped *n* and *p* type, were mounted close to each other, and measured simultaneously, thus ensuring similar amounts of metal deposition, and the exclusion of extraneous shifts due to differences in photon energy, etc. Nominal metal layer thicknesses were measured by a quartz microbalance. The reference level for the photoelectron spectra (the Fermi energy of the

electron analyzer) was measured by recording the valence band spectrum of a gold foil in contact with the sample, which was cleaned *in situ* by scraping with a stainless steel blade. The photon energy was measured to within 0.05 eV from core level emission excited by the second order light from the diffraction grating, and was carefully fixed for each experiment.

III. INTERFACE CHEMISTRY: RESULTS AND DISCUSSION

A. Al/GaP(110): A reactive interface photoemission

Consider first the reaction of Al with GaP(110). A cation exchange reaction has been found in many previous studies of aluminium interaction with (110) surfaces of the III-V semiconductors,⁶⁻⁹ through the emergence of a core level photoemission peak of the cation species (In, Ga) which gave evidence for metallic Ga or In. That a similar reaction takes place in Al/GaP(110) can be observed from the series of room temperature (RT) deposition spectra shown on the left-hand side of Fig. 1. The clean surface spectrum shows the Ga 3*d* bulk doublet along with clear evidence for surface core level emission at higher binding energies, which agrees in magnitude with a recent report.¹⁰ In order to determine the influence of Al deposition on the surface Fermi level from the lowest coverages, doses from 0.007 Å equivalent were used, but here we only show spectra for 0.2 Å or higher because no effects were discernible on the Ga 3*d* peak below this dose. We observe that the valley between the two spin-orbit partners is filled up, and a slight broadening of the peaks occurs. At 0.8 Å aluminium, the broadening has increased, and a shoulder grows at lower binding energy. This feature grows further (5.5 Å) and eventually gives rise to

two sharp peaks located at about 0.9 eV towards lower binding energies, with a slightly larger spin-orbit splitting than the bulk Ga emission; its intensity at 11 Å Al is about 2/3 of the bulk Ga emission. Data by Chiaradia *et al.*¹² for Al/GaP(110), recorded with lower resolution, also show a new feature at lower binding energy at similar depositions. From Fig. 1, it is obvious that the growth of the new feature occurs at roughly constant binding energy. At low temperature (LT, about 100 K), the spectra are very similar at intermediate coverages, but the evolution of intensity and energy is markedly different (right-hand side of Fig. 1). At the highest coverages shown, the peak from GaP still dominates the spectrum at RT, whereas it is almost fully suppressed in the spectra recorded at LT (the low temperature spectrum was recorded at a slightly higher Al dose, but this certainly cannot explain the observed intensity differences). It is also clear from the spectra at lower doses that the binding energy of the new peak exhibits a shift (third and fourth spectrum from bottom) as a function of deposition. At those depositions at which the new peak is prominent or even dominates, one can recognize that its shape is quite different from that of the GaP substrate; the most striking difference is a marked asymmetry towards higher binding energies, which is the signature of the Doniach-Sunjc line shape characteristic of emission from metallic species.¹¹ We therefore identify the new component as metallic Ga produced by the surface or interface reaction between Al and GaP(110). The different line shape is also evident from the line shape analysis shown in Fig. 3 and discussed below.

The occurrence of such a species, and the coverage- and temperature-dependent behavior of its intensity and binding energy complement similar findings for Al deposition on GaAs(110)²⁰ and InP(110).²¹ The interpretation of these results, which in our view also applies to the present case of GaP(110), can be summarized as follows: deposition of Al on the surface of III-V semiconductors causes a cation exchange reaction, driving out Ga atoms which arrange on the surface in the form of three-dimensional islands or clusters. The notion that this reaction is suppressed at low temperature [put forward for Al/GaAs(110)⁶] cannot be reconciled with the strong metallic Ga peaks shown in Fig. 1, and also reported for GaAs and InP. What is changed by lowering the substrate temperature, however, is the morphology of the process. At low temperatures, diffusion of the liberated Ga is strongly reduced, such that the Ga islands may be smaller, and once the exchange reaction is completed, being hindered by the reacted layer, the deposited Al will grow on the surface in a more laminar fashion. The inhibition of Ga diffusion can be derived from the spectrum in Fig. 1. If we assume similar rates for the exchange reaction, the amount of metallic Ga should be about equal in the topmost spectra. The much higher intensity in the metallic Ga peak at LT can be interpreted as being due to smaller clusters covering a larger fraction of the surface, whereas larger clusters leave a major part of the surface uncovered. Also, if the clusters grow beyond a mean diameter larger than twice or three times the electron mean free path λ (under our conditions of extreme surface sensitivity $\lambda \sim 5$ Å), not all reacted material will be detected by the photoemission technique. Thus the

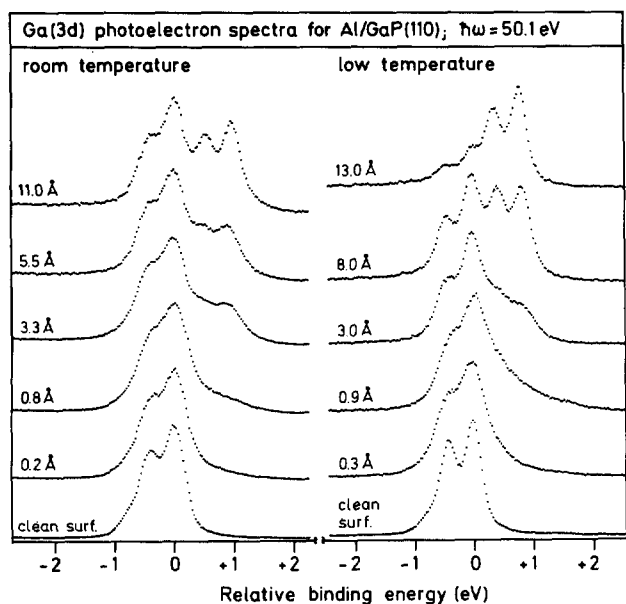


FIG. 1. Set of Ga 3*d* spectra for Al deposition on cleaved GaP(110) surfaces at room and low (~ 100 K) temperatures, recorded at a photon energy of $\hbar\omega = 50.1$ eV, for different doses of Al. Band bending shifts were removed, and spectra were normalized to the same height such that chemical shifts and line shape changes can be more easily detected. Energies are referred to the energy of the Ga 3*d*_{5/2} peak.

difference in intensities of the peak from GaP and metallic Ga can be readily explained on the basis of the reaction and diffusion model. In view of the different growth morphologies a recent claim that in Al/GaAs(110) the amount of released Ga is actually greater for 60 K deposition than at RT is therefore probably difficult to quantify.¹³

This model is further supported by the set of Al 2*p* core level spectra, shown for identical Al depositions at RT and LT in Fig. 2. At room temperature, the initial stages of deposition give rise to a broad featureless peak extending over about 2 eV. Here, the changeover to a metallic state of the aluminium overlayer is readily distinguished by the two sharp peaks due to the 2*p* spin-orbit doublet, already visible at 3.3 Å, but clearly established beyond this deposition; they also have the characteristic asymmetric line shape as demonstrated by the top spectrum on the right-hand side. At low temperature, the reacted peak is much narrower, and the growth of the metallic lines occurs on top of this peak rather than at lower binding energy as observed at RT. The changeover from reacted to metallic species occurs at the same deposition at both temperatures; at this stage, much less material has reacted at LT, most likely due to the fact that the reacted layer is more homogeneous at LT than at RT, such that a thinner layer is already sufficient to act as diffusion barrier. An analysis of the line shape of the reacted aluminium peak is difficult in view of its rather broad and diffuse shape, and the reacted and metallic components can be distinguished without numerical analysis by direct visual inspection in any case; a discussion of the detailed behavior of this interface as a function of metal dose and substrate temperature will be reported elsewhere.¹⁴ At any rate, the broad peak which occurs at low dose is difficult to reconcile with a "stoichiometric" exchange reaction Al + GaP

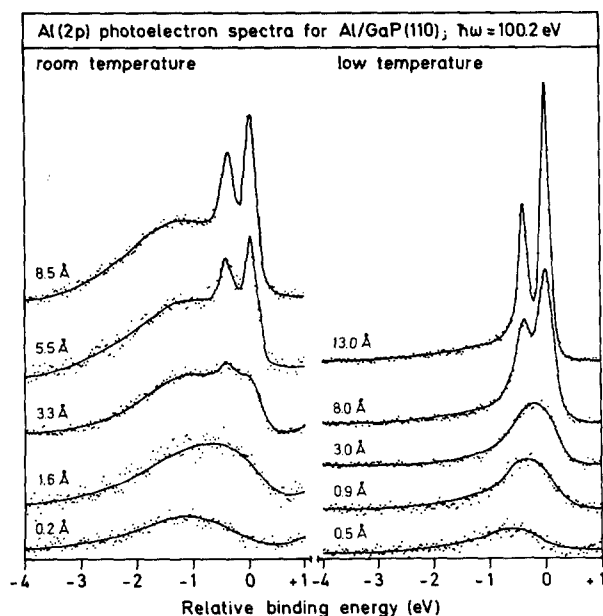


FIG. 2. Set of Al 2*p* spectra for Al deposition on cleaved GaP(110) surfaces at room and low (~ 100 K) temperatures, recorded at a photon energy of $\hbar\omega = 100.2$ eV, for different doses of Al. Band bending shifts were removed, and energies are referred to the energy of the Al 2*p*_{3/2} peak. Within each experiment, spectra were normalized to the photon flux.

\rightarrow AlP + Ga; its width (even a spin-orbit splitting cannot be discerned) suggests a multitude of bonding configurations. This is in line with the loss of crystalline order in the surface as judged from the disappearance of the LEED pattern.

For the Ga 3*d* peak, additional information can be obtained through line shape analysis, and this is shown for two different coverages of Al in Fig. 3, recorded for equal coverages such that a direct comparison is possible. In order to achieve a reasonable line fit, four different spin-orbit doublets were needed. These were modeled by Lorentzians (with a width related to the lifetime broadening) convoluted by a Gaussian representing the instrumental broadening and other broadening effects such as inhomogeneous pinning. The parameters for each doublet (intensity, peak position, Gaussian half-width, and asymmetry) were subjected to a least-squares optimization based on the Marquardt algorithm.¹⁵ For all coverages, the values for the spin-orbit splitting (0.44 eV) branching ratio (0.66), and Lorentzian full width at half-maximum (FWHM) (0.15 eV) of the four components were held constant. Two of the components (the main peak and a component at higher binding energies, both drawn as lines) correspond to the surface and bulk emission on GaP(110), while the other two account for emission from new species caused by the Al-GaP interaction. Up to 0.01 Å of nominal Al coverage, only the bulk and surface substrate components are detected, the latter evident by a shoulder towards higher binding energy (Fig. 1). Their relative position is consistent with the reported surface core level shift of Ga(3*d*) in GaP(110), i.e., $0.32 + 0.02$ eV to higher binding energies.¹⁰ The values of the Gaussian full width at half-maximum (FWHM) of both components in this coverage regime (0.22 eV typically) were similar as those of the clean surface. At progressively higher Al coverages they become broader (FWHM increases up to 0.32 eV), and two new components, shifted to lower binding energies develop, shown by the hatched and shaded curve, respectively.

The shifts of these two new components with respect to the bulk emission are found to be nearly independent of the metal coverage, and are very similar at RT and at LT, in contrast to what has been reported for Al on InP(110).⁶ The

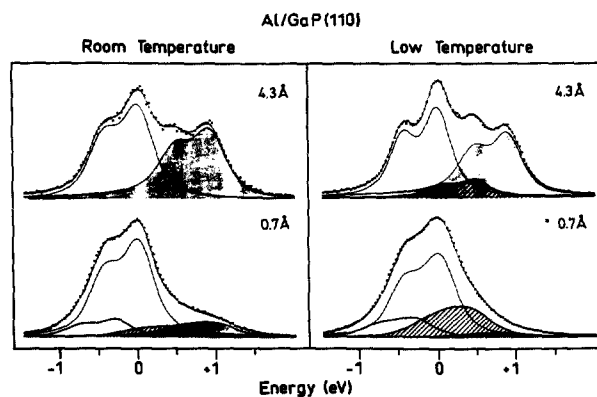


FIG. 3. Line shape analysis of the Ga 3*d* core level region for two doses of aluminium on GaP(110) at room and low temperatures, recorded at $\hbar\omega = 50.1$ eV. Doublets drawn as lines are bulk and surface Ga emission, hatched component is interface Ga, and shaded component is due to elemental (metallic) Ga (see the text).

component with the highest shift appears in Fig. 3 as a shaded area. The value of the shift (0.9–0.95 eV) indicates that it is associated with elemental (henceforth called “metallic”) Ga, liberated in the Al–Ga exchange reaction. The fourth component (named “interface” Ga), with a characteristic shift of $0.40 + 0.05$ eV, appears on the figures as a hatched area. It seems to be an interface related feature, since its contribution is more pronounced at intermediate metal coverages; at room temperature and 4.3 Å metal coverage, it cannot be discerned. This fact and the lower shift are probably the reasons why its presence may not be noticed in a simple visual inspection of the raw data, whereas it appears very clearly in the least-squares line shape analysis. A similar component has been also recently observed in high resolution photoemission studies of Fe/GaAs(110)¹⁶ and In/GaP(110).¹⁷ While the component associated with elemental Ga exhibits the characteristic *D–S* asymmetry of metals,¹¹ particularly obvious in the two upper spectra, the interface feature does not. Also, a distinctly different evolution of the broadening with metal deposition is observed for these two components. The elemental Ga component becomes better resolved with increasing Al deposition. Its Gaussian FWHM sharpens at high Al coverages to values around 100 meV, close to the experimental resolution, indicating a well defined environment. In contrast, the interface component is always very broad. Its Gaussian FWHM is typically 0.5 eV, which suggests that this component contains contributions from interface atoms bonded in different chemical configurations.

The evolution of these two species with Al deposition is found to be clearly dependent on the substrate temperature. The component representing elemental Ga liberated in the exchange reaction is only observed at RT for Al coverages larger than 0.2 Å. At LT however, a higher dose is necessary to detect its presence. Considering this component as a monitor for the cation exchange reaction, it seems that the onset of the reaction is actually retarded by lowering the temperature, although the effect is not very strong. Such onsets should be understood as “apparent onsets,” since the Al doses required in both cases are very small. The fact that no emission from the elemental or metallic Ga component can be distinguished before these coverages may then be simply due to experimental limitations. Keeping in mind this consideration, what our results unambiguously indicate is that the replacement reaction proceeds more slowly at LT. The intensity dependence of the elemental Ga component with metal coverage further confirms such conclusion, since its maximum intensity is reached at 2 Å of nominal Al coverage for RT, and at 3 Å for LT. The lower value obtained at LT may be due to several reasons: a real reduction of the disruptive reaction, a smaller tendency of the exchanged Ga atoms to segregate at the free surface, and/or to the different growth mode of the metal adlayer. Once the maximum is reached, the intensity stays nearly constant at RT, being slightly attenuated at LT. This different attenuation may probably be explained in terms of the different adlayer growth mode. At RT, the elemental Ga liberated from the substrate segregates to the free surface, presumably forming metallic clusters, either between the Al islands or floating on

top of them, and therefore its signal suffers no attenuation.¹⁴ Temperature studies on other reactive interfaces have reported that at LT the released cation atoms are kinetically trapped at the buried interface.¹⁸ This can be ruled out for the Al/GaP(110) system on the basis of our results. Data for Al coverages of more than 5 Å show that the attenuation of the elemental Ga component at LT is substantially lower than that of the Ga 3*d* signal from bulk GaP. It indicates that the “metallic” phase Ga atoms released at LT are not buried at the interface, but located somewhere closer to the surface.

The interface feature of the Ga 3*d* spectrum is clearly stronger at LT than at RT (compare the lower spectra in Fig. 3), in contrast to what happens with the component attributed to metallic gallium. At room temperature the interface feature is in fact very weak. It can only be detected for Al coverages of more than 0.2 Å, i.e., simultaneously with the component due to the exchange reaction. Its highest intensity, which is in fact found at Al coverages of about 0.7 Å, amounts to only 25% of the maximum signal from segregated elemental Ga. Thereafter, its intensity decreases very quickly with metal deposition (much faster than the corresponding substrate bulk signal), so that it cannot be seen for Al coverages higher than 3 Å. At low temperature, however, the behavior of the interface component is very different. Its presence can be detected at Al coverages as low as 0.07 Å, even before the exchanged Ga (Fig. 1). Then it grows very quickly and reaches a maximum at about 0.7 Å. Its contribution is clearly significant at LT as evident from the line shape analysis of Fig. 3. Its maximum signal is more than twice than at RT, and for Al coverages less than 2 Å its intensity is higher than the one from segregated Ga. As was already mentioned, the interface component is only relevant at intermediate coverages. For Al depositions exceeding 1 Å it decreases gradually in intensity, being negligible at high coverages (more than 7 Å). This attenuation is found to be quite similar to that of the substrate bulk peak.

All these observations seem to confirm the hypothesis that the Ga 3*d* “interface” species represents the contribution of Ga atoms in contact with Al adatoms but *not exchanged with them*. Such Ga atoms would be located just at the metal/semiconductor interface, presumably below the Al clusters. This would explain why the signal is higher at LT (where the Al growth is more laminar), increases as the Al atoms cover the substrate surface, and is attenuated as is the substrate signal. For the RT regime, where Al clustering is more pronounced, the number of Ga atoms from GaP in contact with Al would be obviously lower, and also their contribution would be more quickly attenuated than the substrate signal as Al islands grow in size. From our data at RT it is also possible that, for Al coverages higher than 0.7 Å, the exchange reaction affects Ga atoms that initially contributed to the interface species.

B. Examples of unreactive interfaces: In/GaP(110) and Ag/GaP(110)

Having identified the species which lead to the appearance of the photoemission features in the reaction of Al with GaP(110), let us turn to the In/GaP and Ag/GaP systems.

These two metals are considered largely unreactive, such that less drastic changes in the spectra are expected; however, Vitomirov *et al.*¹⁸ have argued that a small amount of Ga is in fact liberated from the substrate, on the basis of Ga 3*d* line shape analysis for room temperature data. Some of our data on this system have already been reported,¹⁷ thus we restrict ourselves to a few representative results, and concentrate on the question whether the core level photoemission data for this system recorded at RT and LT can in fact be interpreted in terms of limited In–Ga exchange reaction. Consider first the RT Ga 3*d* spectra for two different indium coverages shown in Fig. 4. Due to the proximity of the Ga 3*d* and In 4*d* peak, any additional features [such as the reacted species in the case of Al/GaP(110)] may be obscured. However, we can utilize the opportunity provided by a synchrotron radiation source to tune the photon energy, and the differences in photoionization cross section for these levels. The In 4*d* level exhibits a Cooper minimum in the cross section; at $\hbar\omega \sim 50$ eV, its cross section is about 8 times higher than that of the Ga 3*d* level, but for $\hbar\omega \sim 100$ eV, it drops to only 1/10 of the Ga 3*d* cross section.¹⁹ This is shown by a comparison of the spectra shown in Fig. 4, particularly in those for 8 Å In deposition. The In 4*d* peaks are appreciably more intense than the Ga 3*d* ones at 54.1 eV, but at $\hbar\omega = 108.2$ eV (these data actually being recorded using the

second order radiation from the monochromator grating) they have dropped by a factor of 9. Consider the emission in the valley between the Ga and In peaks (about 0.7 eV towards lower binding energies with respect to the Ga 3*d*_{5/2} line), in which also some intensity seems to occur, although it is difficult to judge without line shape analysis whether or not it is due to the tailing of the asymmetric In metal peak. Now the change in intensity also occurs in the valley between the In and Ga peaks; this behavior is also evident for the lower coverage (2 Å, bottom spectra). It is obvious that the extra emission in the “valley” decreases with the indium peaks, and there is no sign of emission due to Ga-related features; our conclusion is thus that no exchange reaction can be inferred from the room temperature deposition data of In/GaP(110), contrary to the model put forward by Vitomirov *et al.*¹⁸

Spectra for In deposition at low temperature complement these findings. Consider the data recorded for different doses at LT in Fig. 5. As in the case of Al/GaP(110) we note a much quicker decrease of Ga 3*d* intensity with In deposition in the spectra recorded with $\hbar\omega = 54.1$ eV, the causes of which certainly lie in the changed morphology as discussed for Al. However, another change compared with the spectra in Fig. 4 is in the shape of the valley between the In and Ga peaks. This has become much more structured, and at intermediate depositions (6 Å) a faint shoulder peak on the Ga 3*d* can be discerned; at higher depositions (12 Å) the Ga

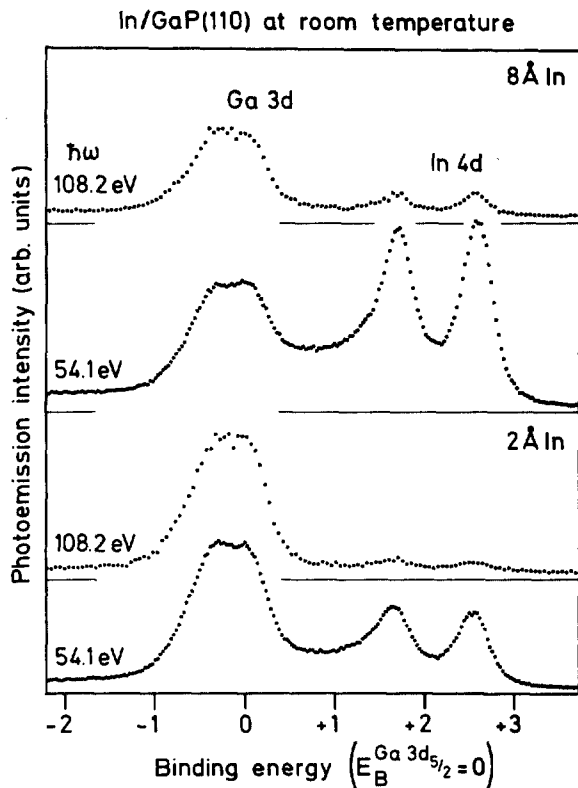


FIG. 4. Ga 3*d* and In 4*d* core level region recorded at $\hbar\omega = 54.1$ eV and $\hbar\omega = 108.2$ eV, for indium deposition on GaP(110) at room temperature and for two selected coverages. Note the simultaneous decrease of the In 4*d* intensity and of the emission in the valley between Ga 3*d* and In 4*d* peaks for $\hbar\omega = 108.2$ eV, and the absence of any new Ga feature in the valley. Spectra were normalized to emphasize changes in the line shape, and band bending shifts were compensated for.

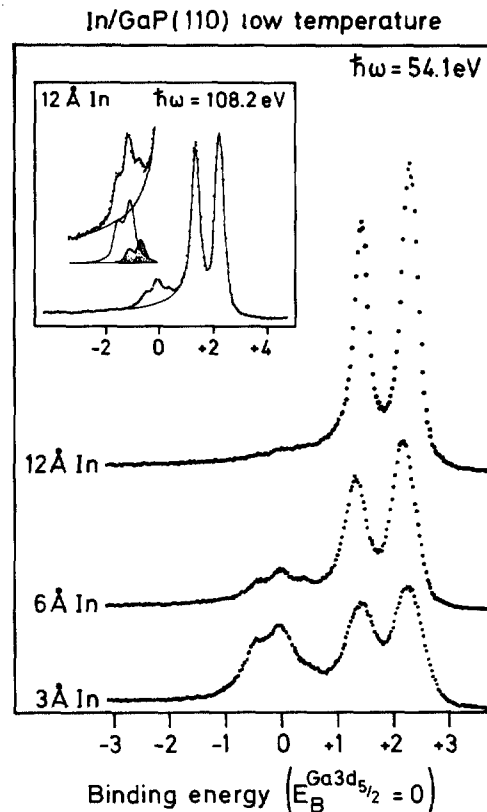


FIG. 5. Ga 3*d* spectra for three doses of In on GaP(110), recorded at $\hbar\omega = 54.1$ eV at low temperature. The inset shows the final dose (12 Å) recorded at $\hbar\omega = 108.1$ eV, where the interface Ga species is visible due to the reduction in intensity of the In 4*d* line doublet. For an explanation of the line shape analysis, see the text.

signal is too faint to detect any structure. It is still quite prominent in spectra recorded at higher photon energies by virtue of the Cooper minimum discussed above as shown in the inset of Fig. 5. A numerical line shape analysis such as carried out for the case of Al/GaP(110), and also displayed in the inset of Fig. 5, reveals the finer details. It is immediately clear that the extra emission originates from a Ga species, because of the spin-orbit splitting which is very similar. We have studied this species over a range of depositions, and found that it is usually quite faint, and only reaches its maximum intensity (less than one monolayer equivalent) at low temperatures and intermediate coverages, just as the interface Ga feature discussed in the data of Al/GaP(110) above. This result suggests that the extra emission, which is shifted with respect to the bulk Ga emission by 0.37 eV towards lower binding energies, is not related to a species resulting from an interface chemical reaction, since one would expect a larger signal as in the case of Al/GaP above. An interpretation in terms of metallic Ga is also unlikely from the binding energy of the peak, and the peak shape which can be readily shown not to be asymmetric.¹⁷ It is also unreasonable to assume that a metallic, exchanged Ga species would be more intense at LT than at RT, as is seen for the shifted peak in the data of Figs. 4 and 5. We interpret the new peak as due to surface Ga atoms which are in contact with deposited In atoms similar to the component found for Al/GaP above. The line shift with respect to the bulk level could well be due to a final state effect, the hole on the surface Ga atom being more effectively screened by the neighboring In atoms. This interpretation of the feature as an interface species is also in accord with the temperature behavior; at low temperature, with a more smoothly growing In film, more of the surface Ga atoms in contact with the In overlayer are "visible" on photoelectron spectroscopy. Thus In/GaP(110) can be considered as a truly unreactive interface; an examination of the P 2*p* level would be helpful in support of this interpretation, but even in the case of the strongly reactive Al/GaP there was very little change in the shape of the P 2*p* line.¹⁴

From previous results for Ag/GaAs(110)²⁰ and Ag/InP(110),²¹ one would expect very little sign for interface reactions also for the system Ag/GaP(110).²² This is borne out by the data for the Ga 3*d* and Ag 4*d* and valence level for room temperature deposition shown in Fig. 6. The Ga 3*d* peak shows very little sign of change, except for some broadening and filling of the slight valley between the *d*_{3/2} and *d*_{5/2} peaks at depositions of 11.5 Å and beyond. The shifts shown here at these depositions are related to the changes in band bending discussed below. The Ag 4*d* and valence region spectra are not normalized to the photon flux here in order to display low deposition features more clearly. At 1.4 Å Ag, a broad peak from the GaP valence band is still prominent in the spectra; it is attenuated upon further doses, and the features in the Ag *d* band develop into sharper structures.

IV. SURFACE FERMI LEVEL POSITION AND SCHOTTKY BARRIER HEIGHTS

According to the interpretation of the core level photoemission results described above, aluminium overlayers on

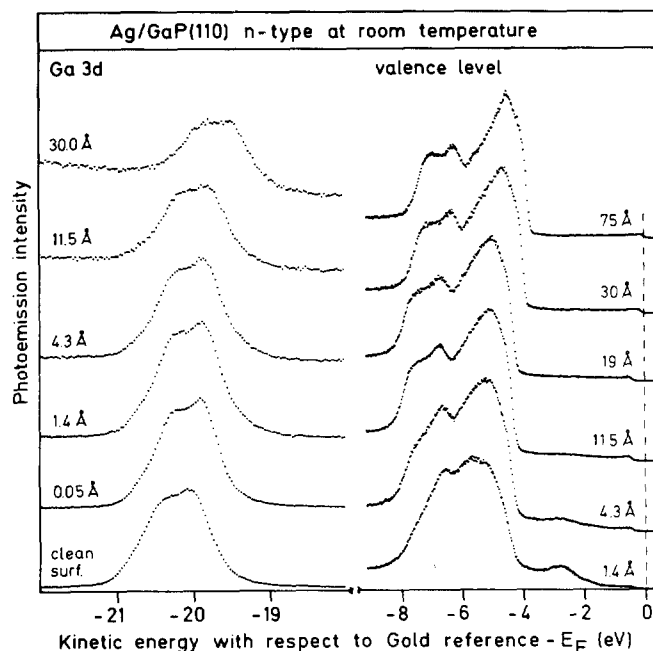


FIG. 6. Sets of spectra for different doses of Ag on *n*-type GaP(110) deposited at room temperature, showing the Ga 3*d* region as well as the valence band region. Spectra were normalized to the same height to emphasize line shape changes.

GaP(110) induce a strong interface reaction while In and Ag overlayers do not. This strong difference in reactivity may have an effect on the coverage dependence of the surface Fermi level, at least for thin overlayers,^{23,24} and the study of surface Fermi level as a function of metal dose is in any case important, since it allows us to determine the Schottky barrier height ϕ_b , the principal parameter of interest in such junctions. We will first discuss Ag overlayers, because an interesting effect was observed in the course of these experiments, which concerns the application of photoelectron spectroscopy for the determination of ϕ_b in general. The usual procedure for obtaining ϕ_b is to determine the precise binding energy of a sharp core level with respect to the valence band maximum (VBM), and to measure the initial position of the VBM with respect to the reference level in the photoemission experiment, usually by recording a metallic Fermi level. The energy shifts in the VBM and thus in the surface Fermi level can then be derived from shifts in the core level, which can be seen up to high coverages when the VBM is totally obscured by emission from the metal overlayer. This method assumes that the photons used for ionization do not disturb the charge equilibrium in the semiconductor. For the present case of Ag/GaP, this assumption is not a valid one as shown by the set of valence band spectra in Fig. 7, recorded for various Ag coverages deposited at room temperature. The clean surface VBM of (*n*-type) GaP(110) has the Fermi level pinned at about 1.8 eV above VBM, most likely due to the empty surface state identified by Drube *et al.*²⁵ Depositions of Ag lead to the appearance of a metallic Fermi edge, still slightly broadened due to island size effects at 4.8 Å Ag, but sharp and intense at 19 Å. What is unusual is the shift of this edge by an amount $\Delta_n = 0.5$ eV towards lower binding energies with respect to the reference Fermi

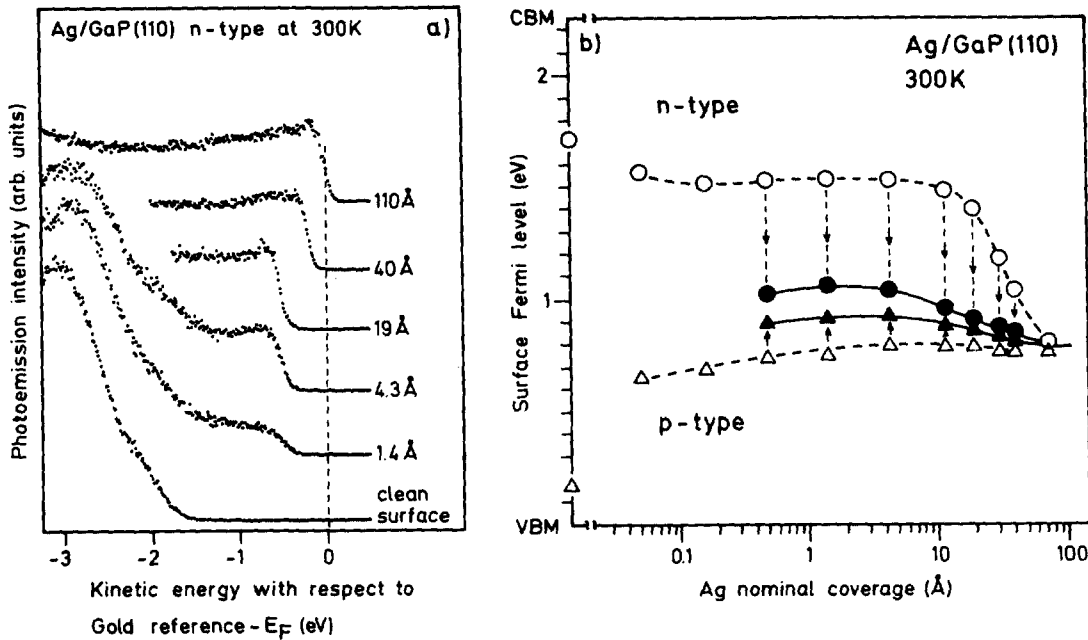


FIG. 7. (a) Valence band maximum region of GaP(110) covered with different doses of Ag at room temperature as indicated. The dashed line gives the energy of the gold Fermi edge used as a reference. Note the gradual shift with coverage of the Ag Fermi edge towards this energy, indicative of the influence of a surface photovoltage (SPV). (b) Position of the surface Fermi level within the band gap as a function of metal dose in Ag/GaP(110). Open symbols were derived from shifts of the Ga 3d core level spectra, while full symbols give data corrected for the surface photovoltage effect shown in (a); corrections Δ_n and Δ_p are shown by arrows.

level. For *p*-type substrates, the Fermi edge emission of the Ag overlayers appears shifted by Δ_p above the reference level emission. The total distance $\Delta = \Delta_p + \Delta_n$ is found to coincide closely with the distance between the Ga 3d core level lines. This indicates the existence of a shift different in sign for the two doping types and equally affecting emission features from both overlayer and substrate. We can exclude charging as a source for the shifts, as checked in experiments on the clean surface; it is also incompatible with the observed shifts because of the opposite sign of Δ_n and Δ_p . This fact also rules out charging of the metal clusters such as observed for Ag on graphite by Wertheim *et al.*²⁶ Similar results were obtained for In and Al overlayers on GaP(110) as discussed below. The shifts Δ_n and Δ_p demonstrate that in the surface layer, a nonequilibrium situation is present. As reported elsewhere,²⁷ we contend that the shifts are due to the presence of a surface photovoltage (SPV),^{28,29} caused by the incident light used for photoexcitation. The mechanism for this process is as follows. In an equilibrium situation, the presence of the metallic overlayer is assumed to give rise to a surface band bending V_{bb} .¹⁻³ The creation of electron-hole pairs by the incident light and/or secondary processes will lead to a nonequilibrium situation if recombination can be neglected. The potential difference V_{bb} causes the electrons to be driven into the bulk, whereas the holes are trapped near the surface, compensating the space charge, and producing a rigid shift of all semiconductor and metal levels. It thus accounts for the occurrence of the overlayer metal Fermi edge at lower (or, for *p*-type material, at higher) energy than the reference Fermi level. This local charge compensation reduces the band bending caused by the metal overlayer. This is a self-limiting process since the surface band bending is needed to separate or trap the mobile carriers. Such effects have previously been observed in photoemission from semiconductor surfaces through *secondary illumination* by high power visible or near-ultraviolet light sources by Margaritondo *et al.*³⁰ Similar phenomena, induced by the light

source used for photoexcitation itself, have been reported in photoemission experiments with Si surfaces at low temperatures by Demuth *et al.*³¹ Previous investigations have shown that its magnitude depends on photon flux, surface recombination, and band bending. SPV increases exponentially with E_g/kT , where E_g is the fundamental gap width.^{28,32} For clean silicon surfaces, Demuth *et al.*³¹ were able to completely compensate the band bending solely by irradiation with the UV source used for photoionization, by lowering the substrate temperature (to below 50 K), which drastically reduces carrier recombination. This suggests that, while recombination has to be suppressed by lowering the temperature in clean silicon ($E_g = 1.12$ eV) in order to observe the SPV effect, the phenomenon can be observed at room temperature in Ag-covered GaP(110) ($E_g = 2.25$ eV) as shown by the data in Fig. 1. For metal-covered semiconductors, the study of Ag on *n*-type CdTe(100) by John *et al.*³³ also reports a shift of the Fermi level in the photoelectron spectrum, although in the opposite direction from that found here. Hecht³⁴ has recently presented calculations which suggest that surface photovoltage effects may be reasonable for differences in Fermi level pinning behavior observed for room temperature and low temperature deposition onto GaAs(110). These calculations would explain recent photoemission results by Aldao *et al.*³⁶ which showed a strong temperature and doping dependence of the band bending induced by Ti, Co, and Ag on GaAs(110). Aldao *et al.* explained their results in terms of a (ground state) "dynamic coupling model" which involves quantum mechanical coupling between metal adatoms and the semiconductor substrate beyond the depletion region. It appears that these results can be explained quite simply in terms of a surface photovoltage (a photoemission final state process) which becomes important in GaAs at lower temperatures, thereby creating the observed differences. This reinterpretation of low temperature band bending results may also be relevant to the large number of studies of other metals on GaAs and

InP surfaces, and to the interpretation of differences in band bending for n - and p -type substrates.²³ These issues are discussed in a more detailed report on SPV effects in photoemission.²⁷

The large SPV observed here in photoelectron spectroscopy from Ag overlayers on GaP(110), and its persistence up to very high metal depositions (it is still clearly visible at a dose of 40 Å Ag equivalent) in particular, has obvious consequences for the determination of temperature-dependent surface band bending and Schottky barrier height. From the data such as shown on the left-hand side of Fig. 7, we derive the surface Fermi level in the manner described above for both n - and p -type material. The corresponding data are shown on the right-hand side of Fig. 7. Open symbols denote the uncorrected data points evaluated without taking account for the nonequilibrium situation, while filled symbols indicate the data after correction for the surface photovoltage; the corrections (Δ_n and Δ_p) are shown by arrows. Note that photoemission will not yield reasonable values about band bending at coverages when a Fermi edge has not been established, such that the correction Δ_n and Δ_p cannot be evaluated. The uncorrected values show the large difference between Fermi level position for n - and p -type substrates over a wide range of depositions. Correction by the SPV yields quite a different picture: the Fermi level positions are quite close even at low depositions, and are within less than 100 meV once the sharp Fermi edge has evolved. For the present purpose of Schottky barrier height determination it is also important to note that the final Fermi level position is only established at very high depositions, where substrate emission is barely detectable (minimum layer thickness more than 30 Å). If we were to base the determination of the Schottky barrier height ϕ_b on coverages as low as 10 or 20 Å, the final value would be missed. This may be one reason why the Schottky barrier for Ag on n -type GaP(110) derived here ($\phi_b = 1.5$ eV) differs appreciably from that reported by Chiaradia *et al.* ($\phi_b = 1.08$ eV).¹²

Figure 8 shows similar data for Ag and In overlayers recorded at low substrate temperature. The surface Fermi level data points have the same meaning as in Fig. 7 as far as corrections for surface photovoltage are concerned. For Ag, we observe even larger corrections for Δ_n (up to 0.9 eV), somewhat large than at room temperature for Δ_p , and the establishing of a metallic Fermi level emission at lower depositions as expected from the discussion of overlayer morphology above. The final LT value for ϕ_b is within 100 meV of the room temperature value which is also given in the figure for comparison. In the lower part of Fig. 8, the data for indium exhibit a very similar trend, with large corrections for SPV up to 20 Å. The low temperature value for ϕ_b again agrees well with the room RT value.

It has been argued that reactive and unreactive metal-semiconductor interfaces may exhibit differences in the way the surface Fermi level depends on the amount of metal deposited, and such differences have in fact been found at room and low temperatures.²³ Our study of surface Fermi level movement in Al/GaP reveals that there are no strong differences between the surface Fermi level dependence for Al on the one hand and In or Ag on the other. This can be derived

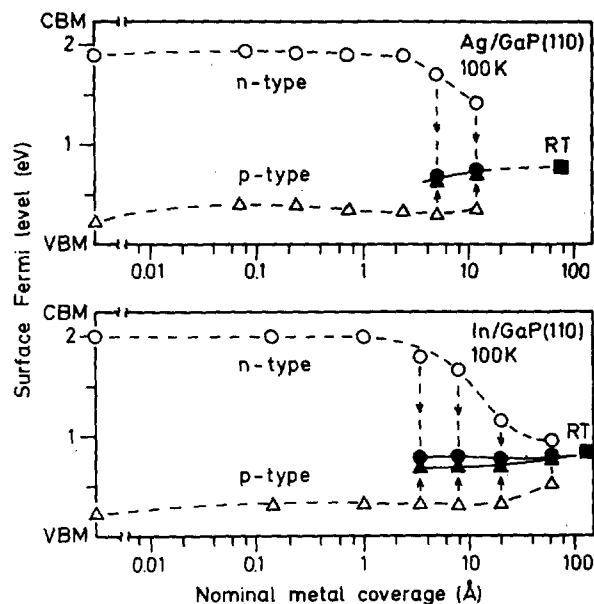


FIG. 8. Position of surface Fermi level as a function of metal dose for Ag/GaP(110) (upper panel) and In/GaP(110) at low temperature. In both cases, considerable shifts due to a surface photovoltage occur, indicated by the arrows (see the text). For both metals, the final room temperature pinning level is also shown. Open and full symbols have the same meaning as in Fig. 7.

from the LT data in Fig. 9. The uncorrected data points would indicate that very little change in the position of the Fermi level occurs as a function of coverage for either n - and p -type substrates. As mentioned above, the SPV corrections can only be applied once a metallic Fermi edge is obtained from the overlayer, which in case of Al occurs at about 5 Å. At this stage the Fermi levels are actually found to coincide,

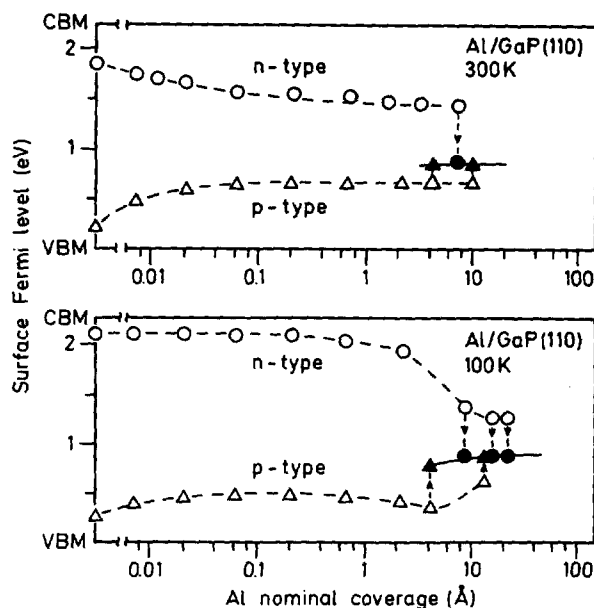


FIG. 9. Same as Fig. 8 but for Al/GaP(110) at room temperature (upper panel) and at low temperature (lower panel). In both cases, noticeable shifts due to surface photovoltage occur, indicated by the arrows (see the text). The final pinning position is found to be the same in both cases.

such that no further movement occurs. The data for room temperature deposition of Al, which are somewhat more complicated due to the clustering processes will be reported elsewhere.

From the data contained in Figs. 7, 8, and 9, the value of the Schottky barrier height ϕ_b for the three metals on *n*-type GaP(110) can be compared. The values are $\phi_b^{\text{Ag}} = 1.50$ eV, $\phi_b^{\text{In}} = 1.32$ eV, and $\phi_b^{\text{Al}} = 1.37$ eV. These data deviate strongly from values previously found for these metals on GaP(110) by photoelectron spectroscopy by Chiaradia *et al.*,¹² for the case of In/GaP(110) by about 1 eV. These workers recorded the Schottky barrier height for metals which span a work function range of about 1 eV, and found a linear behavior of Schottky barrier height with metal work function, and concluded that for different metals on GaP(110), the "Schottky limit" applied.² For many other semiconductor substrates, including the widely studied GaAs(110), current thinking relates Schottky barrier height with the action of metal-induced (or virtual) gap states (MIGS or ViGS), which, by being filled with electrons up to a specific charge neutrality level (CNL), dominate the establishment of the Schottky barrier.^{1-3,23} This concept, while being modified at low coverages where metal-induced donors²³ or metal-induced defects may play a role in Fermi level pinning, is widely regarded as providing the correct explanation for the experimental observation that the pinning position of the Fermi level for a wide variety of metals on many semiconductors is restricted to a small range of energies. Thus a clear-cut example of the opposite behavior, the dependence of ϕ_b on metal work function predicted by Schottky and Mott, is most interesting since it might reveal the limits for the midgap theories.

The reasons for the discrepancy between our data and those of Chiaradia *et al.*¹² are not clear at present. We have shown above that surface photovoltage influences the determination of ϕ_b , even at room temperature; however, the effect of SPV, leading to flatband conditions at intermediate coverages, would tend to narrow the range of band bending, in contrast to what was found by Chiaradia *et al.* The final pinning values used by Chiaradia *et al.* were for room temperature deposition, and for depositions of 20 Å equivalent. Here, according to the data presented in Fig. 7 (room temperature Ag) we are still away from the final value by more than 0.45 eV. For this situation it appears likely that the SPV-induced shifts influence the determination of ϕ_b . They certainly have wider and more general implications for the study of coverage-dependent band bending induced by metal overlayers on semiconductors by photoemission.

ACKNOWLEDGMENTS

We gratefully acknowledge the expert help of H. Haak in the preparation of the crystals, C. Stephens for the preparation of the Al MBE cell, as well as the support by the BESSY staff. This work was supported by Bundesministerium für Forschung und Technologie under Grant No. 05 490 FXB as well as the Deutsche Forschungsgemeinschaft through SFB 6 project A 05.

- ^{a)} Istituto di Struttura della Materia-CNR, I-00044 Frascati-Roma, Italy.
^{b)} Sektion Chemie der Karl-Marx-Universität Leipzig, DDR-7010 Leipzig.
^{c)} BESSY GmbH, Lentzeallee 100, D-1000 Berlin 33, West Germany.
¹ L. J. Brillson, *Surf. Sci. Rep.* **2**, 123 (1982).
² E. H. Rhoderick and R. H. Williams, *Metal-Semiconductor Contacts*, 2nd ed. (Clarendon, Oxford, 1988).
³ L. J. Brillson and G. Margaritondo, in *The Chemical Physics of Solid Surfaces and Heterogeneous Catalysis*, edited by D. A. King and D. P. Woodruff (Elsevier, Amsterdam, 1988), Vol. 5.
⁴ L. J. Brillson, M. L. Slade, R. E. Viturro, P. Chiaradia, D. Kilday, M. K. Kelly, and G. Margaritondo, *Appl. Phys. Lett.* **39**, 1379 (1987).
⁵ H. Haak, W. G. Wilke, and K. Horn (to be published).
⁶ K. Stiles, A. Kahn, D. G. Kilday, and G. Margaritondo, *J. Vac. Sci. Technol. B* **5** 987 (1987), and references therein.
⁷ R. Cao, K. Miyano, T. Kendelewicz, K. K. Chin, I. Lindau, and W. E. Spicer, *J. Vac. Sci. Technol. B* **5**, 998 (1987).
⁸ T. Kendelewicz, W. G. Petro, I. A. Babalola, J. A. Silberman, I. Lindau, and W. E. Spicer, *J. Vac. Sci. Technol. B* **1**, 623 (1983).
⁹ A. B. McLean, I. T. McGovern, C. Stephens, W. G. Wilke, H. Haak, K. Horn, and W. Braun, *Phys. Rev. B* **38**, 6330 (1988).
¹⁰ A. B. McLean and R. Ludeke, *Phys. Rev. B* **39**, 6223 (1989).
¹¹ S. B. Doniach and M. Sunjic, *J. Phys. C* **3**, 285 (1970).
¹² P. Chiaradia, L. J. Brillson, M. Slade, R. E. Viturro, D. Kilday, N. Tache, M. Kelly, and G. Margaritondo, *J. Vac. Sci. Technol. B* **5**, 1075 (1987); P. Chiaradia, M. Fanfoni, P. Nataletti, P. DE Padova, R. E. Viturro, and L. J. Brillson, *ibid.* **7**, 195 (1989).
¹³ S. G. Anderson, C. M. Aldao, G. D. Waddill, I. M. Vitomirov, S. J. Severtson, and J. H. Weaver, *Phys. Rev. B* **40**, 8305 (1989).
¹⁴ M. Alonso, R. Cimino, Th. Chassé, and K. Horn (to be published).
¹⁵ P. R. Bevington, *Data Analysis and Error Reduction in the Physical Sciences* (McGraw-Hill, New York, 1968).
¹⁶ R. Cimino, C. Carbone, and W. Braun, Proceedings of the 7th International Vacuum Congress, Köln 1989 [Vacuum (to be published)].
¹⁷ Th. Chassé, M. Alonso, R. Cimino, K. Horn, and W. Braun, Proceedings of the 7th International Vacuum Congress, Köln 1989 [Vacuum (to be published)].
¹⁸ I. M. Vitomirov, C. M. Aldao, M. Schabel, G. D. Waddill, S. G. Anderson, and J. H. Weaver, *J. Vac. Sci. Technol. A* **7**, 758 (1989).
¹⁹ J. J. Yeh and I. Lindau, *At. Data. Nucl. Data Tables* **32**, 1 (1985).
²⁰ D. Bolmont, P. Chen, F. Proix, and C. Sebenne, *J. Phys.* **15**, 3639 (1982); R. Ludeke, T.-C. Chiang, and T. Miller, *J. Vac. Sci. Technol. B* **1**, 581 (1983).
²¹ I. A. Babalola, W. G. Petro, T. Kendelewicz, I. Lindau, and W. E. Spicer, *Phys. Rev. B* **29**, 6614 (1984).
²² B. M. Trafos, F. Xu, M. Vos, C. M. Aldao, and J. H. Weaver, *Phys. Rev. B* **40**, 4022 (1989).
²³ W. Mönch, *J. Vac. Sci. Technol. B* **6**, 1270 (1988).
²⁴ W. Mönch, *Europhysics Lett.* **7**, 275 (1988).
²⁵ D. Straub, M. Skibowski, and F. J. Himpsel, *J. Vac. Sci. Technol. A* **3**, 1484 (1985).
²⁶ G. K. Wertheim, S. B. DiCenzo, and S. E. Youngquist, *Phys. Rev. Lett.* **51**, 2310 (1983).
²⁷ M. Alonso, R. Cimino, and K. Horn, *Phys. Rev. Lett.* **64**, 1947 (1990).
²⁸ H. C. Gatos and J. Lagowski, *J. Vac. Sci. Technol.* **10**, 130 (1973).
²⁹ G. Heiland and H. Lüth, *Nuovo Cimento B* **39**, 748 (1977).
³⁰ J. E. Demuth, W. J. Thompson, N. J. DiNardo, and R. Imbihl, *Phys. Rev. Lett.* **56**, 1408 (1986).
³¹ G. Margaritondo, L. J. Brillson, and N. G. Stoffel, *Solid State Commun.* **35**, 277 (1980).
³² S. M. Sze, *Physics of Semiconductor Devices*, 2nd ed. (Wiley, New York, 1982).
³³ P. John, T. Miller, T. C. Hsieh, A. P. Shapiro, A. L. Wachs, and T.-C. Chiang, *Phys. Rev. B* **34**, 6704 (1986).
³⁴ M. Hecht, *Phys. Rev. B* **41**, 7918 (1990); *J. Vac. Sci. Technol. B* **8**, 1018 (1990).
³⁵ C. M. Aldao, S. G. Anderson, C. Capasso, I. M. Vitomirov, G. D. Waddill, and J. H. Weaver, *Phys. Rev. B* **39**, 12977 (1989); I. M. Vitomirov, G. D. Waddill, C. M. Aldao, S. G. Anderson, C. Capasso, and J. H. Weaver, *ibid.* **39**, 3483 (1989).